Faculty of Science

DEVELOPMENT AND VALIDATION OF qPCR TARGETS FOR *PORPHYROMONAS GINGIVALIS* ABUNDANCE AND THE EXPRESSION LEVELS OF GENES IN THE HUMAN ORAL MICROBIOME

2023 | JULIANA KAITLYN HERMISTON

B.Sc. HONOURS THESIS - BIOLOGY

THOMPSON RIVERS UNIVERSITY

DEVELOPMENT AND VALIDATION OF qPCR TARGETS FOR *Porphyromonas gingivalis* ABUNDANCE AND THE EXPRESSION LEVELS OF GENES IN THE HUMAN ORAL MICROBIOME

by

JULIANA KAITLYN HERMISTON

A THESIS SUBMITTED IN PARTIAL FULFILLMENT

OF THE REQUIREMENT FOR THE DEGREE OF

BACHELOR OF SCIENCE (HONS.)

in the

DEPARTMENT OF BIOLOGICAL SCIENCES

(Cellular, Molecular, Microbial Biology)

THOMPSON RIVERS UNIVERSITY

This thesis has been accepted as conforming to the required standards by:

Eric M. Bottos (Ph.D.), Thesis Supervisor, Dept. Biological Sciences

Mark E. Rakobowchuk (Ph.D.), Co-supervisor, Dept. Biological Sciences

Jonathan D. Van Hamme (Ph.D.), Co-Supervisor, Dept. Biological Sciences

Matthew Reudink (Ph.D.), External Committee Member, Dept. Biological Sciences

Dated this 5th day of May, 2023, in Kamloops, British Columbia, Canada

ABSTRACT

Porphyromonas gingivalis is a pathogen found in patients with periodontitis that produces toxic cysteine proteases called gingipains. Gingipains are characterized as narrow-spectrum virulence targets. Broad-spectrum antibiotics do not eliminate *P. gingivalis* but, instead, add to its resistance. Sometimes found in the brains of Alzheimer's patients, it has been suggested that *P. gingivalis*, and the gingipains it produces, is involved in cognitive decline. Specifically, lysine-gingipan and arginine gingipain A and B are crucial to the pathogenicity of *P. gingivalis* and are involved in host colonization, suppression of host defenses, nutrient acquisition, and tissue destruction. It has been found that inhibiting gingipain production decreases *P. gingivalis* brain colonization, reducing neurodegeneration in Alzheimer's disease. Similarly, it has been suggested that dietary nitrate supplementation may limit *P. gingivalis* proliferation. The work presented here builds on a clinical trial where participants were given nitrate pills and monitored for changes in oral microbiome community composition. Twenty human oral microbiome RNA samples were subjected to reverse transcriptase quantitative PCR (RT-qPCR) analysis to quantify the abundance of *P. gingivalis* and the expression levels of genes involved in gingipain production, iron acquisition from host heme, as well as nitrate metabolism. This study designed and validated primers and probes for qPCR for *hmuY*, *kgp*, and *narG*. We found that *hmuY*, *kgp*, and *narG* were amplified of correct size in the positive control samples (100 ng/µL stock *P. gingivalis*, AlphaDNA), suggesting that the primer targets are accurate. This work will lay foundation for quantifying the absolute abundance of *P. gingivalis* and the expression levels of *hmuY*, *kgp*, and *narG* in the cDNA samples using qPCR, and, overall, how nitrate supplementation affects these abundances. Additionally, results from the qPCR analysis will give us more precise measurements of how much *Porphyromonas sp.* are present in the samples which can then be compared to the

physiological responses to nitrate supplementation from the study conducted by Freeze et al. (2022). It is hypothesized that reduction in the expression of gingipains and iron acquisition genes, and an increase in the expression of nitrate reductase genes, post nitrate supplementation, will correlate with reduced *P. gingivalis* abundance.

Thesis Supervisors: Drs. Eric M. Bottos, Mark E. Rakobowchuk, and Jonathan D. Van Hamme

ACKNOWLEDGEMENTS

I would first like to thank the participants who volunteered to take part in this study, many of them being students, friends, and professors at TRU.

Thank you to my friends and family for always supporting my goals and supporting me throughout each stage of the research process. A very special thank you to my friend Natalie Pietramala for holding my hand throughout undergrad and for your never-ending encouragement.

Thank you to Ashley Fischer and Breanne McAmmond for being incredible mentors during my time in the TRUGen lab; the mentorship laid the foundation for my research journey. Your encouragement and support are forever appreciated, and I am certain that the experience would not have been the same without you both.

I would like to extend my utmost gratitude towards Gwen Freeze. Thank you for being such a positive light in my life. It was a privilege to walk alongside you for this project, and your continued support and encouragement is more appreciated than words can describe. You are an inspiration for many! Even miles apart, I've never felt more loved and supported.

Thank you to Dr. Mark Rakobowchuk for your constant support and encouragement throughout the entirety of the project. The care and attention you have put into this project as well as your undying support of my research journey will be forever appreciated.

Thank you to Dr. Jon Van Hamme for your endless support of my research endevours. The opportunities that I have had during my time in the TRUGen lab are ubiquitous, and I have gained countless skills that I will undoubtedly take into my future career. Your support for not only my research journey but my academic career as a whole is beyond appreciated.

Finally, thank you to Dr. Eric Bottos for being such a supportive and encouraging mentor throughout this project. Your dedication to your students does not go unnoticed. The countless hours you spent with me in the lab and the many skills that you have taught me are greatly appreciated. Thank you for making this such an invaluable experience.

TABLE OF CONTENTS

LIST OF FIGURES

LIST OF TABLES

1 INTRODUCTION

1.1 Alzheimer's disease

Alzheimer's disease (AD) is a neurogenerative disease characterized by its gradual decline in cognitive function, specifically in brain areas that are responsible for learning and memory (Kametani and Hasegawa 2018; Raji 2009; Anand and Dhikav 2012). As the most common form of dementia, AD has been studied for several decades; however, the pathogenesis of this disease remains poorly understood (Santos et al. 2017). Risk factors contributing to the development of AD, such as aging, genetic predisposition, immune dysfunction, and poor cardiovascular health, have been well established, but currently there are no methods of treatment to prevent or cure the disease (Armstrong 2013; Santos et al. 2017). Two abnormal structures called amyloid-ß (Aß) plaques and neurofibrillary tangles (NFTs) found in the brain have distinguished AD from other neurodegenerative diseases (Glenner and Wong 1984; Grundle-Iqbal et al. 1986). Aß plaques are made up of Aß peptide chains whereas NFTs are accumulations of hyperphosphorylated tau proteins (d'Errico and Meyer-Luehmann 2020). Research has shown that the accumulation of these structures, specifically in the hippocampus and entorhinal cortex regions of the brain, directly damages neural synapses (d'Errico and Meyer-Luehmann 2020).

1.1.1 Amyloid-ß plaques

Amyloid-ß (Aß), a product of the glycoprotein amyloid precursor transmembrane protein found in brain tissue, regulates neuron growth, synaptic functions, neuroprotection, as well as mediates nervous system development (Chen et al. 2017; d'Errico and Meyer-Luehmann 2020). In a healthy individual, Aß monomers are formed in the brain and released into the extracellular space where they are either degraded or transported out of the organ (Chen et al. 2017). Contrastingly, in persons with AD, Aβ aggregates into soluble oligomers that can accumulate in

the brain, driving synaptic dysfunction, or into larger insoluble amyloid fibrils that can form plaques (d'Errico and Meyer-Luehmann 2020; Chen et al. 2017). Research suggests that Aβ plaque formation plays a role in AD pathogenesis by inducing neuronal loss, synaptic dysfunction, and disrupting neural connectivity (d'Errico and Meyer-Luehmann 2020; Chen et al. 2017; Murphy and Levine 2010). The mechanism by which this occurs remains unclear however existing hypotheses allude to the abnormal tendency of Aß to aggregate into plaques, or the important role that Aß plays as an antimicrobial peptide (Kumar et al. 2017).

More recently, Aß as an antimicrobial peptide that protects the host from microbial invasion has been studied (Kumar et al. 2017; Gosztyla et al. 2018). Aß functions by binding and intercepting microorganisms from entering neurons; this reduces microbial adhesion to host cells and eventually kills bacteria (Kumar et al. 2017). Despite the protective nature of Aß, studies have suggested that it can become dysregulated in response to microbial invasion and cause inflammation, host cell toxicity, and degenerative pathologies such as ones seen in AD (Kumar et al. 2017). Therefore, the accumulation of Aß plaques in AD patients may be a result of an overactive innate immune system in the brain in response to microbial invasion (Kumar et al. 2017).

1.1.2 Neurofibrillary tangles and tau protein

Like Aß plaques, neurofibrillary tangles (NFTs) may also play an important role in the pathogenesis of AD. NFTs are composed of filaments of the microtubule-associated phosphoprotein, tau – a protein responsible for microtubule assembly and stability (Kametani and Hasegawa 2018). In AD, the tau protein becomes hyperphosphorylated, causing the microtubules to disassemble and release the tau protein (d'Errico and Meyer-Luehmann 2020; Medeiros et al. 2011). The tau proteins then aggregate within the cytosol and inhibit normal neuronal signalling

viability (d'Errico and Meyer-Luehmann 2020). Healthy cells may take up the tau aggregates or they can be transferred via synapses and quickly invade healthy brain areas (d'Errico and Meyer-Luehmann 2020).

Even though there is substantial evidence supporting the Aß and NFT hypotheses as hallmark drivers of AD, studies have recently highlighted other mechanisms that may play an important role in AD etiology. Increasing evidence suggests that cardiovascular health and, more recently, oral health play an integral role in AD pathogenesis (de Bruijn and Ikram 2014; Kelleher and Soiza 2013; Ide et al. 2016).

1.2 Proliferation of *Porphyromonas gingivalis* in the oral cavity

The exact mechanism by which oral health is involved in AD pathology is not well known. Multiple studies have found periodontal disease to be closely linked to the development of AD (Ide et al. 2016; Dominy et al. 2019; Beydoun et al. 2020). Periodontal disease, also known as gum disease, is one of the most widespread diseases in westernized countries, including North America, and is thought to be the leading cause of tooth loss in older populations (Ide et al. 2016). It is a gum infection that damages the tissues surrounding the teeth, due to the dysbiosis of the commensal oral bacteria that leads to inflammation of the gingiva, the breakdown of connective tissue, and the formation of periodontal pockets (Kinane et al. 2017; Leira et al. 2017). Periodontal pockets are spaces around the teeth underneath the gum line that create an environment that favours the proliferation of bacteria, particularly gram-negative species (Kamer et al. 2008).

Porphyromonas gingivalis is the keystone pathogen found in patients with periodontitis. This bacterium typically exists in commensal harmony with the host; however, it can quickly shift into a disease role if it excessively proliferates in the subgingival dental plaque (Lamont and Jenkinson 1998; Guo et al. 2010). As a gram-negative anaerobic bacterium, *P. gingivalis* produces

toxic cysteine proteases that include lysine-gingipain (Kgp), arginine-gingipain A (RgpA), and arginine-gingipain B (RgpB) (Dominy et al. 2019). Gingipains are characterized as narrow-spectrum virulence targets; broad-spectrum antibiotics do not eliminate *P. gingivalis* and, instead, add to its resistance. Gingipains contribute to 85% of proteolytic tissue destruction and enable a tight adherence to sites in the oral cavity where they can exploit nutrients from- the host such as heme and iron (Dominy et al. 2019; Guo et al. 2010). This increases nutrient delivery to dental plaque communities, sustains chronic inflammation in the host gingival tissue, and induces apoptosis of gingival epithelial cells (Shi et al. 1999; Guo et al. 2010; Stathopoulou et al. 2009; Sheets et al. 2005). Gingipains are crucial in *P. gingivalis* pathology as they exploit host signalling pathways to degrade extracellular protein matrixes, resist death by phagocytes, avoid host-induced apoptosis, and alter the cytokine network to avoid host defence (Guo et al. 2010). Kgp and RgpA/B are crucial to the pathogenicity of *P. gingivalis* and are involved in host colonization, suppression of host defenses, nutrient acquisition, and tissue destruction (Dominy et al. 2019).

1.3 Proliferation of *Porphyromonas gingivalis* in the brain

Levels of this bacterium have also been found in the brains of patients with Alzheimer's disease suggesting that *P. gingivalis,* and the gingipains it produces, are involved in the pathophysiology that leads to cognitive decline in this disease (Dominy et al. 2019; Ide et al. 2016; Poole et al. 2015; Singhrao et al. 2015). *P. gingivalis* residing within periodontal pockets enables it to have easy access to the circulatory system and other parts of the body, such as the brain (Guo et al. 2010). In the brain, *P. gingivalis* moves from neuron to neuron, causing increased infection over time, contributing to AD through several mechanisms (Dominy et al. 2019). The bacterium can alter the function of monocytes and use them to travel to the circulatory system. Furthermore, processes of bacteremia where bacteria can enter the bloodstream from gingival bleeding can also

induce the proliferation of bacteria in the circulatory system (Kanagasingam et al. 2020; Singhrao et al. 2015; Dominy et al. 2019). *P. gingivalis* can then cross the permeable blood-brain barrier and enter the brain via endothelial cells (Singhrao and Harding 2020). Another mechanism by which *P. gingivalis* invasion of the brain may occur is through an olfactory or trigeminal cranial nerve infection (Dominy et al. 2019). Furthermore, research has also suggested that the inflammatory products produced in periodontal disease increase Aß and tau protein production in brain tissue of patients with AD (Kamer et al. 2008; Ishida et al. 2017). Gingipains that are released in the brain can cleave tau proteins therefore altering neuronal functioning and potentially increasing cognitive decline (Dominy et al. 2019).

1.4 Gingipain inhibition

The link between *P. gingivalis* and AD has motivated researchers to try to treat *P. gingivalis* associated AD. Because antibiotics are ineffective in treating *P. gingivalis* invasion, small molecule gingipain inhibitors were developed (Dominy et al. 2019). Dominy et al. (2019) found that directly inhibiting gingipain production using short peptide analogs decreases colonization of the brain by *P. gingivalis*, therefore, reducing neurodegeneration in Alzheimer's disease. Kgp inhibitors have shown promise in reducing the amount and persistence of *P. gingivalis* present in the brains of mice (Dominy et al. 2019). The study demonstrated that gingipain inhibitors can decrease the amount of *P. gingivalis* in the brain, block gingipain-caused neurodegeneration, decrease the Aß host response, and reduce overall neuroinflammation (Dominy et al, 2019). The Kgp inhibitors also block the acquisition of host heme by *P. gingivalis* – a process mediated by a unique hemophore, *hmuY*, that acts as a biomarker for *P. gingivalis* (Smalley et al. 2007).

1.4.1 Nitrate supplementation

Another mechanism that may provide similar effects to that of gingipain inhibitors is the administration of a dietary nitrate supplement. Researchers suggest the oral microbiome may be altered by nitrate/nitrite presence, and the salivary composition can be altered via dietary nitrate supplementation (Vanhatalo et al. 2018). The nitrate-nitrite-nitric oxide pathway relies on bacteria within the oral microbiome to convert nitrate to nitrite, and this pathway may be an important contributing factor to overall health (Vanhatalo et al. 2018). Nitric oxide is a vasodilator that is utilized by the microbes in the oral cavity (Rosier et al. 2020). The production of nitric oxide via nitrate supplementation causes systemic benefits including decreased blood pressure and arterial stiffness, improved endothelial function, and reverses metabolic syndrome (Vanhatalo et al. 2018; Rosier et al. 2020). Likewise, Rosier et al. (2020) suggested that nitrate could be used as a dietary intervention to promote eubiosis in the oral microbiome.

Human cells lack NO_3^- reduction abilities; however, commensal bacteria residing in the oral cavity use NO_3^- as a terminal electron acceptor in their metabolism by reducing NO_3^- to NO_2^- and further to NO through the nitrate-nitrite-nitric reduction pathway (Vanhalato et al. 2018; Dejam et al. 2004). In humans, upon NO_3^- ingestion up to 25% enters enterosalivary circulation where it becomes concentrated in the saliva and anaerobic bacteria in the oral cavity are responhh sible for the reduction of NO_3^- to NO_2^- (Wylie et al. 2013). When the NO_2^- enters the stomach, the acidic environment converts some of the NO_2^- into NO and the rest is absorbed to increase NO_2^- concentration in the circulating blood plasma (Wylie et al. 2013). NO is synthesized from L-arginine by isoforms of the NO synthase and is involved in several important biological functions including vascular tone regulation, immune response, and neurotransmission (Romitelli et al.

2007). Dietary nitrate supplementation can increase nitrite concentration in blood plasma and serum and reduce resting blood pressure (Jones 2014).

In a previous study, we assessed the effects of a dietary nitrate supplementation on oral microbial community composition and overall physiological health in a healthy study population. We hypothesized that a dietary nitrate supplementation would reduce the abundance of *P. gingivalis*, and improve secondary physiological outcomes tied to cardiovascular disease. To test this hypothesis, a 10-day dietary nitrate supplementation was administered using potassium nitrate to ten healthy participants. Using 16S rRNA gene sequencing, shifts in the oral microbial community structure, specifically the abundance of *P. gingivalis*, were assessed, as well as secondary physiological outcomes of blood pressure and endothelial function as markers of cardiovascular disease risk.

Previously conducted studies have yielded promising data in reducing the abundance of *P. gingivalis* present in the oral microbiome which subsequently reduces the production of gingipains. The abundances of four target genes, *kgp, hmuY, NarG* (a nitrate reductase gene), and the *16SrRNA* gene for *P. gingivalis*, will be assessed in the current study. This work will build on a larger study that examined the effect of nitrate supplementation on the abundance of *P. gingivalis* in the oral microbiome and secondary physiological responses. To my knowledge, no other studies have specifically analyzed the *kgp, hmuY, and narG* genes as well as the absolute abundance of *P. gingivalis* in response to in vivo nitrate supplementation. We hypothesize that a reduction of *P. gingivalis* in the oral microbiome could lower the risk of periodontitis and Alzheimer's disease and improve various cardiovascular and physiological responses. If improvements are seen in the aforementioned factors, future studies can be conducted to assess the effects of nitrate

supplementation on those individuals with Alzheimer's disease to see if there is a link between oral microbiome dysbiosis and cognitive impairment.

2 MATERIALS AND METHODS

2.1 Ethical approval

Ethical approval was granted from the Thompson Rivers University Research Ethics Board and Biosafety approval was granted by Thompson Rivers University Biosafety Committee. All participants gave their written and informed consent, both after the experimental procedure and risks had been explained to them and prior to the start of testing.

2.2 Study Participants

Ten healthy participants including seven males and three females between 20-49 years of age were recruited to participate in the study. Recruitment was of Thompson Rivers University professors and students, as to limit contact with the public due to the COVID-19 pandemic at the time of testing. Participants were screened prior to testing to ensure they were suitable study participants. All participants had their initial vaccination for COVID-19 (> 2 weeks prior to testing), no blood or platelet/bleeding disorders, and no known cardiac diseases and/or cardiovascular risk factors. None of the participants were hypertensive, smokers, diabetics, or had other known metabolic diseases. The participants were not taking medication or treatment for any disease, did not experience aversion to the sight of blood and/or needles, and were over 19 years of age and under 49 years of age.

Preceding testing, participants were instructed to arrive at the laboratory rested, having refrained from strenuous physical activity, alcohol, marijuana, or non-prescription drug ingestion 24 hours prior to sampling. They were instructed not to cycle or run to and from the laboratory on

sampling days, nor partake in any physically demanding work in the hours after the sampling day. Participants were asked to avoid caffeine on the day of sampling before their testing, eating within 4 hours prior to sampling, and blood donations eight weeks prior to, and eight weeks after participation. Additional participant exclusion criteria included using antimicrobial or antiseptic tooth paste 48 hours prior to testing, mouthwash 48 hours prior to test, and flossing on the morning of test days, as followed by criteria used in the NIH Human Microbiome Project.

2.3 Experimental Design

Participant testing consisted of blood pressure and ultrasonographic measurements, blood extraction, and oral bacterial sampling, although only oral bacterial sampling is relevant to the current project. Upon arrival to the lab, participants were placed in a supine position in a dimly lit, temperature controlled (21-24°C) room and were instrumented with a non-invasive continuous blood pressure monitor. Once an adequate blood pressure signal was recording, the lights were turned off and the participant was left in a supine position for ten minutes to ensure baseline sampling was taken at rest, with minimal sympathetic nervous system activation.

Oral samples of floss were then taken and later subject to RNA extraction, rt-qPCR, and qPCR to determine expression levels of *kgp, hmuY,* and *narG* genes as well as absolute abundance of *P.* gingivalis. At the end of sampling, participants were given twenty 400 mg potassium nitrate oral supplements to be taken twice a day for the 10 days preceding their post testing. Male participants returned two weeks after their pre-testing for post testing, while females returned 28 days after their pre-testing to control for potential influences of the female menstrual cycle. In both groups, the nitrate supplements were taken in the final 10 days preceding post supplement testing. Upon return for post testing, the same above procedures were repeated.

2.4 Oral Bacteria Sampling

Following blood collection, oral floss samples were collected for microbial analysis, as per methodology outlined in the NIH Human Microbiome Project – Core Microbiome Sampling Protocol and altered where necessary.

2.4.1 Hard tissue floss

A hard tissue gum line sample was obtained by flossing. Participants were instructed to floss four teeth, each twice, with sterile disposable floss picks for a total of eight floss samples. The teeth flossed were between each canine and first premolar in the top right, bottom right, top left, and bottom left areas of the mouth. The floss of each pick was removed with a sterile razor and all eight floss samples were placed together in a 2 mL screw top tube containing 1 g sterile ceramic beads and 600 µL Buffer RLT Plus. If participants bled during flossing, the floss was disposed, and they were instructed to floss between the first and second premolar of the same area instead (e.g., top right). The tube was then flash frozen in liquid nitrogen and stored at -80°C until further DNA analysis.

2.5 RNA Isolation

Hard tissue floss samples from both pre and post nitrate supplementation of the 10 participants were isolated using an AllPrep DNA/RNA Mini Kit (Qiagen, Hilden, Germany). Samples were frozen in Buffer RLT Plus and were stored in tubes containing 1 g of sterile silica beads. Once all samples were thawed, 6 µL of beta-mercaptoethanol (BME) was added to each sample, homogenized by bead beating (vortexing) for 5 minutes, and centrifuged at 8000 rpm for 30 seconds following the methodology outlined by Moen et al. (2016). From then onwards, manufacturer's instructions were followed. Once the RNA had been extracted, it was quantified using a Qubit 2.0 Fluorometer (Invitrogen, Carlsbad, CA, USA).

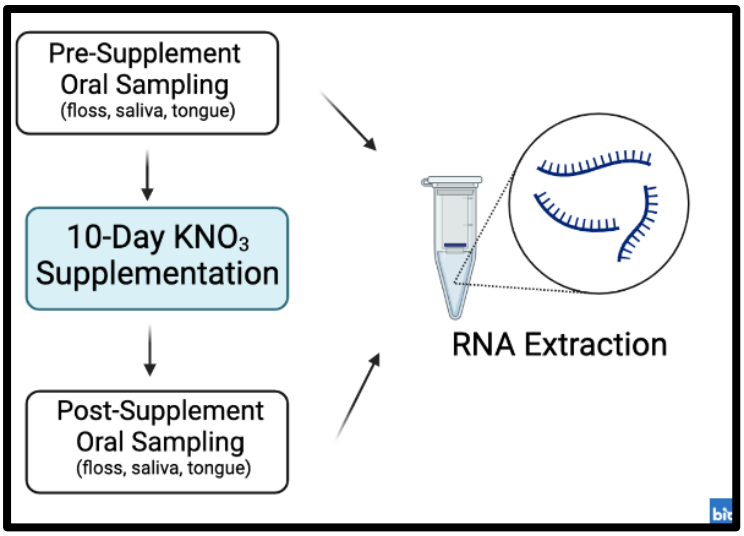

Figure 1. Methodology and timeline showing how the RNA extracts were obtained from the previous study conducted by Freeze et al. (2022).

2.6 RNA Quantification

A quantification of the 20 floss RNA extracts was carried out using the Qubit 2.0 Fluorometer (Invitrogen, Carlsbad, CA, USA) and Qubit™ RNA HS Assay Kit (Thermo Fisher Scientific, Massachusetts, USA).

2.7 Reverse Transcriptase Polymerase Chain Reaction

Reverse transcriptase polymerase chain reaction (RT PCR) was carried out on 20 floss RNA extracts using the SuperScript™ IV VILO™ Master Mix (Invitrogen, Carlsbad, CA, USA). Genomic DNA digests were prepared for each of the samples containing 1 uL 10X ezDNAse buffer, 1 µL ezDNAse enzyme, 6 µL nuclease-free water, and 2.5 µg RNA to a final volume of 10µL in microcentrifuge tubes. The tubes were incubated at 37°C for 2 minutes and subsequently centrifuged and placed on ice. Reverse transcription and non-reverse transcription template controls were prepared using 4 µL SuperScript™ IV VILO™ Master Mix and SuperScript™ IV VILO™ No RT Control respectively and 6 µL nuclease-free water to a final volume of 10 µL in

microcentrifuge tubes. PCR thermocycling conditions included: primer annealing for 10 minutes at 25°C; reverse transcription for 10 minutes at 50°C; and enzyme inactivation for 5 minutes at 85°C. Reverse transcription was assessed in all samples and controls by running 5 μL of product on a 1% agarose gel prepared in TAE buffer, and product sizes were determined by comparison to 500 ng of 1 kb Plus Ladder run on the same gel. The gel was run at 70 volts for 25 minutes and visualized on a UV transilluminator.

2.8 Primer and Probe Design

2.8.1 Acquiring Sequences from the National Centre for Biotechnology Information (NCBI)

For *kgp,* approximately 10 sequences were selected in *P. gingivalis* strains from NCBI and subsequently parsed. BLAST was run to find similar sequences, and the FASTA file was acquired and uploaded to Geneious Prime. For *hmuY,* approximately 10 sequences were selected in *P. gingivalis* strains from NCBI and subsequently parsed. BLAST was run to find similar sequences, and the FASTA file was acquired and uploaded to Geneious Prime. For the *16SrRNA* gene, only 1 sequence for 1 strain of *P. gingivalis* was found on NCBI and BLAST was run to find similar sequences, and the FASTA file was acquired and uploaded to Geneious Prime. For *kgp,* approximately 10 sequences were selected in *P. gingivalis* strains from NCBI and subsequently parsed. BLAST was run to find similar sequences, and the FASTA files were acquired and uploaded to Geneious Prime. For *narG,* approximately 10 sequences were selected and parsed in strains from *Actinomyces*, *Corynebacterium*, *Kingella*, *Rothia,* and *Veillonella*, which were the genera that were most abundant in the DNA samples from the previous study conducted by Freeze et al. (2022). BLAST was run to find similar sequences, and the FASTA files were acquired and uploaded to Geneious Prime.

Table 1. Summary of the four gene targets in which primers and probes will be designed for qPCR.

Target Gene	Target Bacteria	Analysis
16SrRNA	*Porphyromonas gingivalis*	absolute abundance of *P.gingivalis* present in samples
kgp	*Porphyromonas gingivalis*	abundance of gingipains present in samples
hmuY	*Porphyromonas gingivalis*	abundance of iron acquisition genes in samples; *hmuY* codes for a hemophore unique to *P. gingivalis*
narG	*Veillonella sp. Actinomyces sp.*, *Corynebacterium sp.*, *Kingella sp.*, *Rothia sp.*, and *Veillonella sp.*	abundance of nitrate reducing genes present in the samples; measures the expression of nitrate reducers in response to the supplementation

2.8.2 Geneious Prime Software

FASTA files acquired from NCBI were uploaded to Geneious Prime Software and aligned using Multiple Sequence Comparison by Log-Expectation (MUSCLE) parameters. Primers and probes were designed and selected on conserved regions of the genome, as well as based on parameters size as target size of amplicon (50-150bp), length (18-21 nucleotides) melting temperature (60-80°C), and GC content (approximately 50%). Three primer and probe combinations were selected for each of the four genes of interest (Table 1).

2.9 Amplification using Polymerase Chain Reaction

2.9.1 Amplification of the *kgp* gene

Polymerase chain reaction (PCR) of the *kgp* gene was carried out on extracted DNA samples from the previous study (Freeze et al. 2022) to test the targets. A 20 μL reaction mixture was prepared in a microcentrifuge tube containing a final concentration of 1X GoTaq Green Master

Mix (Promega, Madison, USA), 0.05 µM forward primer (80F ATGCTCCGACTACTCGAA, 362F TGCCACATCAACCCTCTA, or 2436F AGGACAGGGTGAAGTTGT), 0.05 µM reverse primer (183R ACCTTTGGTCTCCACCTT, or 437F GCATAAGCAGCAGCATTG, or 2516R CACATCTTTCCGGATGCA), and 2 µL isolated DNA from each sample. In place of the 2 µL DNA sample, 2 µL of *P. gingivalis* stock (AlphaDNA) was used as a positive control and 2 µL of PCR-grade water as a negative control. Each 20 µL reaction mixture was transferred to a well in a 96-well PCR plate and PCR was completed in a SimpliAmp Thermal Cycler (Thermo Fisher Scientific, Massachusetts, USA). PCR thermocycling conditions included: an initial denaturation for 10 minutes at 95°C; 40 cycles of denaturation for 15 seconds at 95°C, primer annealing for 1 minute at 60°C; and a final extension for 5 minutes at 72°C. PCR amplification was assessed in all samples and controls by running 5 µL of product on a 2% agarose gel prepared in TAE buffer, and product sizes were determined by comparison to 500 ng of 1 kb Plus Ladder run on the same gel. The gel was run at 80 volts for 90 minutes and visualized on a UV transilluminator.

2.9.2 Amplification of the *hmuY* gene

Polymerase chain reaction (PCR) of the *hmuY* gene was carried out on extracted DNA samples from the previous study (Freeze et al. 2022) to test the targets. A 20 µL reaction mixture was prepared in a microcentrifuge tube containing a final concentration of 1X GoTaq Green Master Mix (Promega, Madison, USA), 0.05 µM forward primer (384F CCACTTTCGCCACAATTGAGACA, 496F ACTGCCACGTTTCGTATT, or 536F TTTGGTTACTGCTTCGGG), 0.05 µM reverse primer (513R AATACGAAACGTGGCAGTTCG, or 627R TCTGTGCATTGCCATTGA, or 639R TTTTCTCCGCACTCTGTG), and 2 µL isolated DNA from each sample. In place of the 2 µL DNA sample, 2 µL of *P. gingivalis* stock (AlphaDNA) was used as a positive control and 2 µL of

PCR-grade water as a negative control. Each 20 µL reaction mixture was transferred to a well in a 96-well PCR plate and PCR was completed in a SimpliAmp Thermal Cycler (Thermo Fisher Scientific, Massachusetts, USA). PCR thermocycling conditions included:

an initial denaturation for 10 minutes at 95°C; 40 cycles of denaturation for 15 seconds at 95°C, primer annealing for 1 minute at 60°C; and a final extension for 5 minutes at 72°C. PCR amplification was assessed in all samples and controls by running 5 µL of product on a 2% agarose gel prepared in TAE buffer, and product sizes were determined by comparison to 500 ng of 1 kb Plus Ladder run on the same gel. The gel was run at 80 volts for 90 minutes and visualized on a UV transilluminator.

2.9.3 Amplification of the *NarG* gene

Polymerase chain reaction (PCR) of the *narG* gene was carried out on extracted DNA samples from the previous study (Freeze et al. 2022) to test the targets. A 20 µL reaction mixture was prepared in a microcentrifuge tube containing a final concentration of 1X GoTaq Green Master Mix (Promega, Madison, USA), 0.05 µM forward primer (2383F CTGTATGCCGACGTGATT, 2433F CTTGAACACGTCCGACAT, or 3251F CCGCCAGCATTTCTATCA), 0.05 µM reverse primer (2515R CCCAGTCGGATTTGCTTTCCGTG, or 2513R CAGTCGGATTTGCTTTGC, or 3361R TTCATGCCCAGCAGTTTT), and 2 µL isolated DNA from each sample. In place of the 2 µL DNA sample, 2 µL of *P. gingivalis* stock (AlphaDNA) was used as a positive control and 2 µL of PCR-grade water as a negative control. Each 20 µL reaction mixture was transferred to a well in a 96-well PCR plate and PCR was completed in a SimpliAmp Thermal Cycler (Thermo Fisher Scientific, Massachusetts, USA). PCR thermocycling conditions included: an initial denaturation for 10 minutes at 95°C; 40 cycles of denaturation for 15 seconds at 95°C, primer annealing for 1 minute at 60°C; and a final extension for 5 minutes at 72°C. PCR amplification

was assessed in all samples and controls by running 5 µL of product on a 2% agarose gel prepared in TAE buffer, and product sizes were determined by comparison to 500 ng of 1 kb Plus Ladder run on the same gel. The gel was run at 80 volts for 90 minutes and visualized on a UV transilluminator.

2.9.4 Amplification of the *16SrRNA* gene

Polymerase chain reaction (PCR) of the *16SrRNA* gene was carried out on extracted DNA samples from the previous study (Freeze et al. 2022) to test the targets. A 20 µL reaction mixture was prepared in a microcentrifuge tube containing a final concentration of 1X GoTaq Green Master Mix (Promega, Madison, USA), 0.05 µM forward primer (226F TAAGATAGGCATGCGTCC, 582F GTTGTTCGGTAAGTCAGC, or 1177F GGTGTGGATGACGTCAAT), 0.05 µM reverse primer (319R AGTGTGGGGGATAAACCT, or 721R AATCGGAGTTCCTCGTGA, or 1294R TGGGGAAGGGTTTAGAGA), and 2 µL isolated DNA from each sample. In place of the 2 µL DNA sample, 2 µL of *P. gingivalis* stock (AlphaDNA) was used as a positive control and 2 µL of PCR-grade water as a negative control. Each 20 µL reaction mixture was transferred to a well in a 96-well PCR plate and PCR was completed in a SimpliAmp Thermal Cycler (Thermo Fisher Scientific, Massachusetts, USA). PCR thermocycling conditions included: an initial denaturation for 10 minutes at 95°C; 40 cycles of denaturation for 15 seconds at 95°C, primer annealing for 1 minute at 60°C; and a final extension for 5 minutes at 72°C. PCR amplification was assessed in all samples and controls by running 5 µL of product on a 2% agarose gel prepared in TAE buffer, and product sizes were determined by comparison to 500 ng of 1 kb Plus Ladder run on the same gel. The gel was run at 80 volts for 90 minutes and visualized on a UV transilluminator.

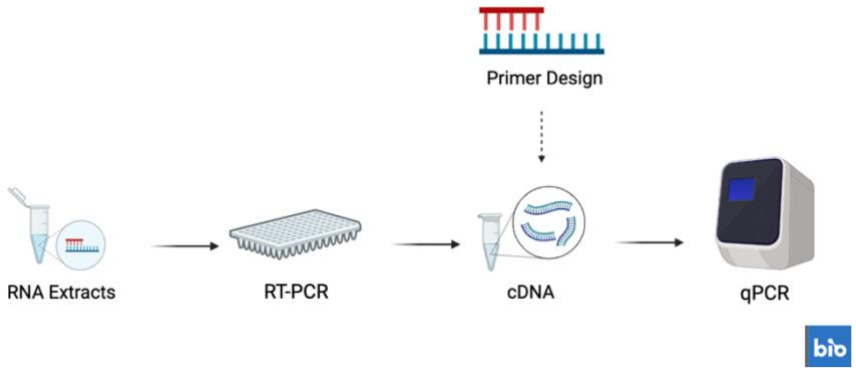

Figure 2. Primers and probes were designed to target regions of the cDNA for subsequent quantitative polymerase chain reaction (qPCR).

3 RESULTS

3.1 Primer and Probe Combinations from Geneious Prime

Primer and probe combinations were designed and specified in Geneious Prime software. Primers and probes were designed and selected on conserved regions of the genome, as well as based on parameters size as target size of amplicon (50-150bp), length (18-21 nucleotides) melting temperature (60-80°C), and GC content (approximately 50%). Three primer and probe combinations were selected for each of the four genes of interest (Table 1).

Table 1. Primer and probe combinations selected for testing using polymerase chain reaction (PCR).

Target Gene	Forward Primer	Probe	Reverse Primer
16SrRNA	226F TAAGATAGGCATGCGTCC	276P AGGCGACGATGGGTAGGGGAA	319R AGTGTGGGGGATAAACCT
	582F GTTGTTCGGTAAGTCAGC	643P CCGGGCTTGAGTTCAGCGGC	721R AATCGGAGTTCCTCGTGA
	1177F GGTGTGGATGACGTCAAT	1236P TGGGAGGGACAATGGGCAGCT	1294R TGGGGAAGGGTTTAGAGA
kgp	80F ATGCTCCGACTACTCGAA	123P GCAGTTCGATGCAAGCTTTTCGTTCA	183R ACCTTTGGTCTCCACCTT
	362F TGCCACATCAACCCTCTA	390P TGATGATCCCGAAAAGGTTCCCTTCGT	437R GCATAAGCAGCAGCATTG
	2436F AGGACAGGGTGAAGTTGT	2457P CCCCGGTGGTGTTTACGACTATTGCA	2516R CACATCTTTCCGGATGCA
hmuY	*384F* CCACTTTCGCCACAATTGAGACA	416P GCGGTGAAGAGCCATGTCCCA	513R AATACGAAACGTGGCAGTTCG
	496F ACTGCCACGTTTCGTATT	556P ACTGCCACGTTTCGTATT	627R TCTGTGCATTGCCATTGA
	536F TTTGGTTACTGCTTCGGG	556P TGGAGGGTTGGTTCGGCTCGT	639R TTTTCTCCGCACTCTGTG
narG	2383F CTGTATGCCGACGTGATT	2438P ACACGTCCGACATGCACCCGT	2515R CCCAGTCGGATTTGCTTTCCGTG
	2433F CTTGAACACGTCCGACAT	2451P GCACCCGTTCATCCACCCGT	2513R CAGTCGGATTTGCTTTGC
	3251F CCGCCAGCATTTCTATCA	3308P TGCCTACCGTCCCGCAGTCG	3361F TTCATGCCCAGCAGTTT

3.2 Reverse Transcriptase Polymerase Chain Reaction

Results from the agarose gels confirm that reverse transcription was successful in all 20 floss samples (10 pre- and 10 post-nitrate supplementation) (Figure 3, 4, 5, & 6). Product sizes were determined in samples and controls by comparing the amplified regions to 500 ng of 1 kb Plus Ladder.

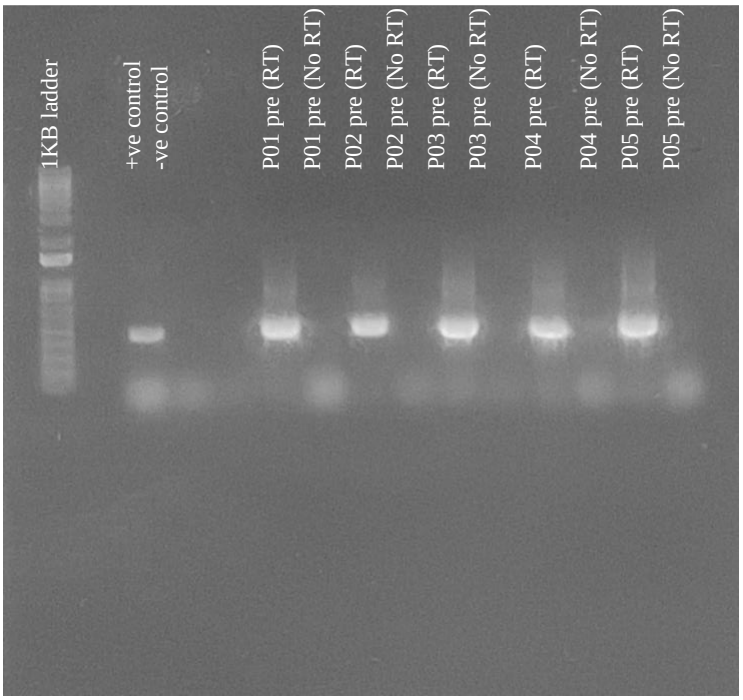

Figure 3. Agarose gel confirming the reverse transcription of the RNA samples (P01pre-P05pre) using reverse transcriptase polymerase chain reaction. +ve = positive; -ve = negative; RT = reverse transcription

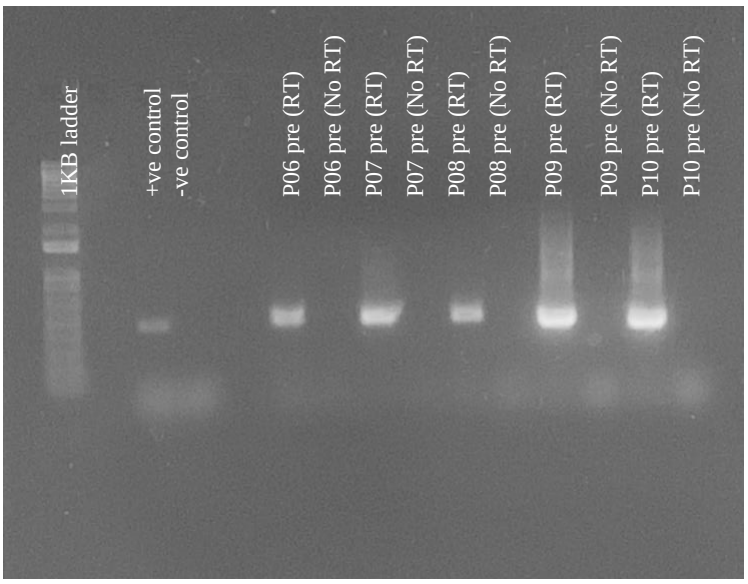

Figure 4. Agarose gel confirming the reverse transcription of the RNA samples (P06pre-P10pre) using reverse transcriptase polymerase chain reaction. +ve = positive; -ve = negative; RT = reverse transcription

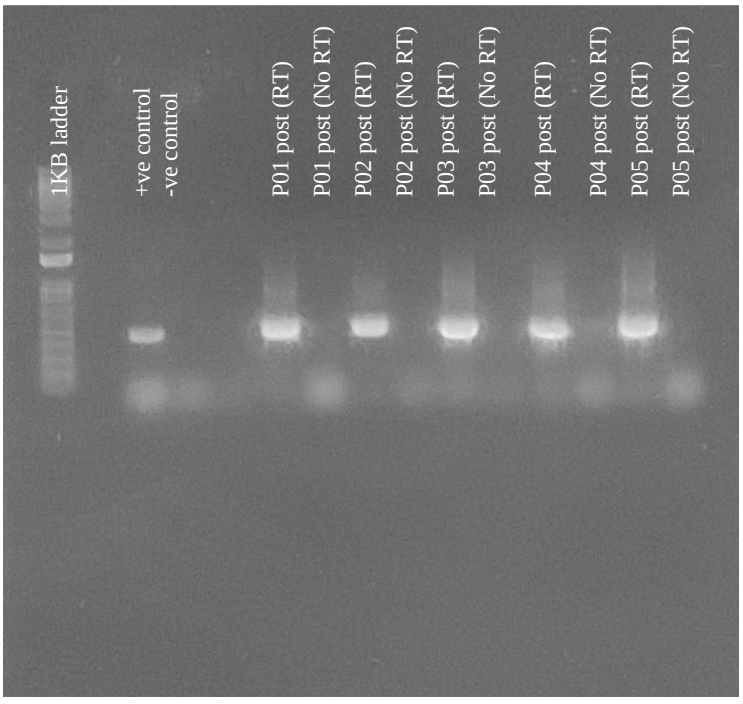

Figure 5. Agarose gel confirming the reverse transcription of the RNA samples (P01post-P05post) using reverse transcriptase polymerase chain reaction. +ve = positive; -ve = negative; RT = reverse transcription

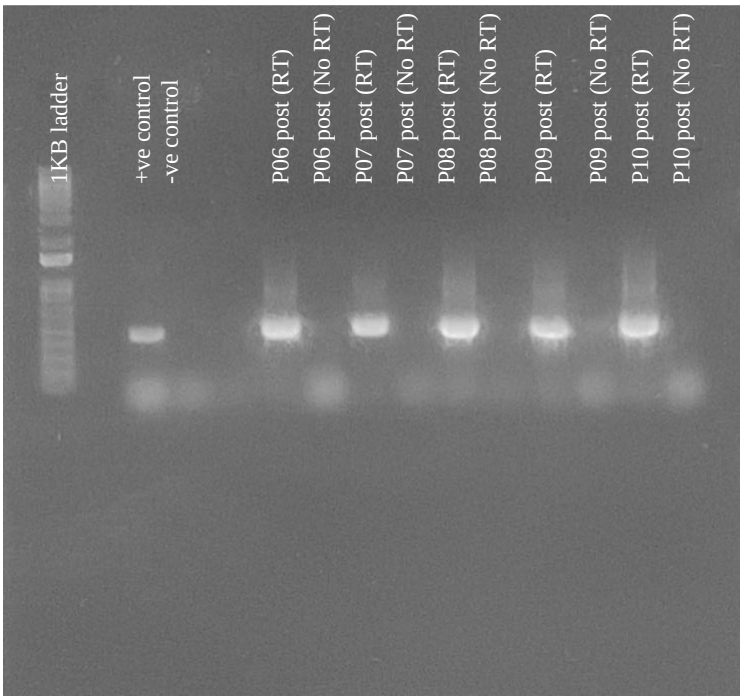

Figure 6. Agarose gel confirming the reverse transcription of the RNA samples (P01post-P05post) using reverse transcriptase polymerase chain reaction. +ve = positive; -ve = negative; RT = reverse transcription

3.3 Primer Combination Testing

3.3.1 *kgp*

Results from the agarose gel shows presence of amplified regions of target sizes in the positive control lanes (*P. gingivalis* stock; Alpha DNA) for all three primer/sets – 80F/183R, 362F/437F, and 2436F/2516R. This suggests that the *kgp* gene was amplified using all three sets. Sanger sequencing on the gel bands can be done to confirm their identity and the specificity of the primers (Figure 7).

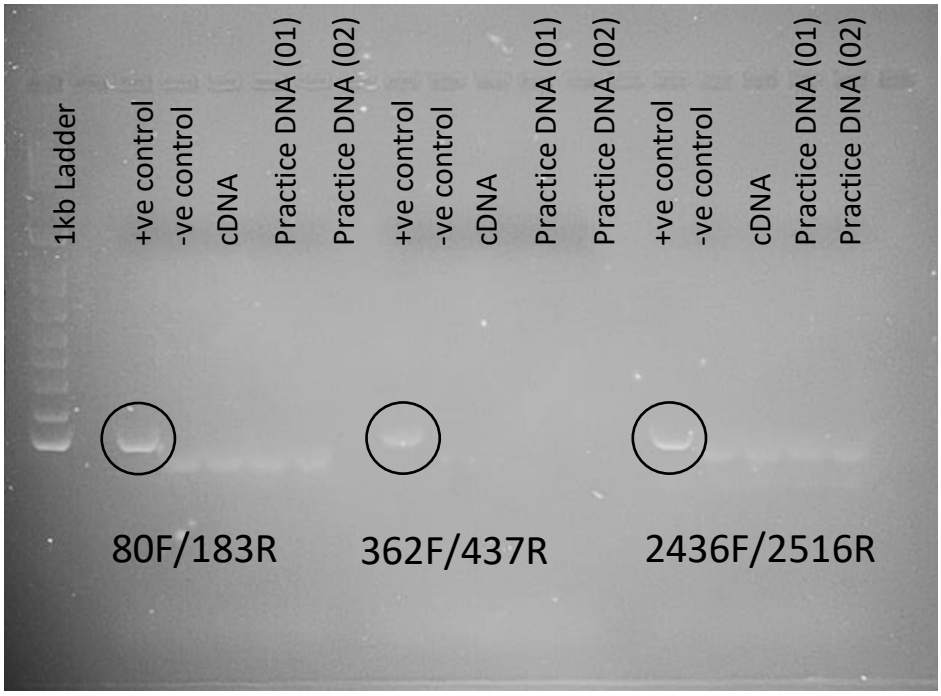

Figure 7. Agarose gel confirming the amplification of *kgp* with the 80F/183R, 362F/437R, and 2436F/2516R primer sets. +ve = positive; -ve = negative

3.3.2 *hmuY*

Results from the agarose gel shows presence of an amplified region of target size in the positive control lane (*P. gingivalis* stock; Alpha DNA) for one of the primer/sets – 384F/513R. This

suggests that the *hmuY* gene was amplified using this set. Sanger sequencing on the gel band can be done to confirm its identity and the specificity of the primers (Figure 8).

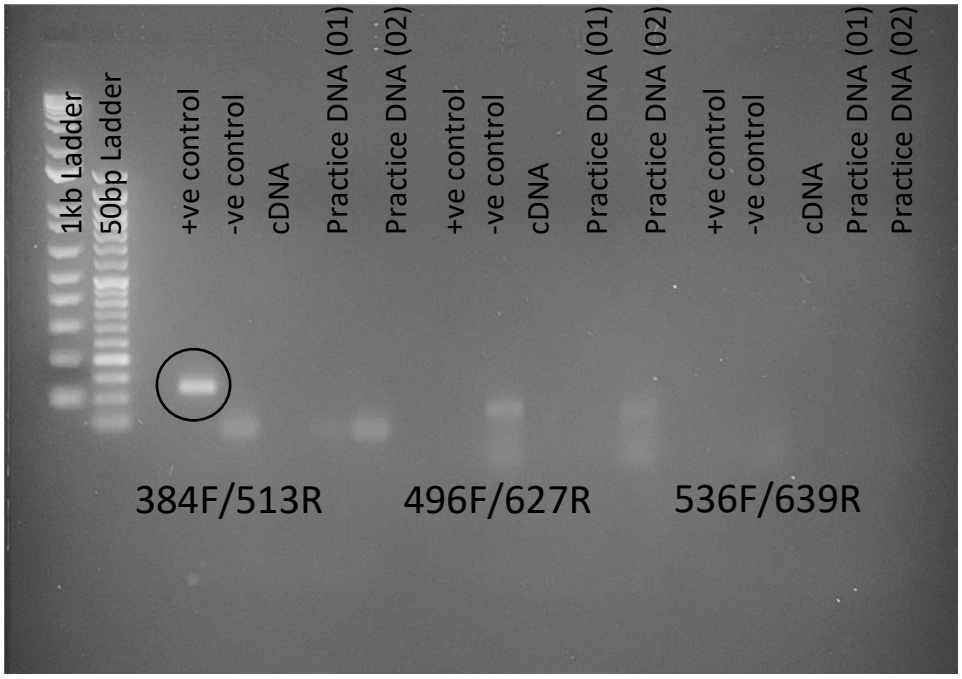

Figure 8. Agarose gel confirming the amplification of *hmuY* with the 384F/513R primer set. +ve = positive; -ve = negative

3.3.3 *narG*

Results from the agarose gel shows presence of an amplified region of target size in the positive control lane (*P. gingivalis* stock; Alpha DNA) for one of the primer/sets – 2383F/2515R. This suggests that the *narG* gene was amplified using this set. Sanger sequencing on the gel band can be done to confirm its identity and the specificity of the primers (Figure 9).

Figure 9. Agarose gel confirming the amplification of *narG* with the 2383F/2515R primer set. +ve = positive; -ve = negative

3.3.4 *16SrRNA*

Results from the agarose gel does not show presence of amplified regions of target size in the positive control lane (*P. gingivalis* stock; Alpha DNA) for any of the primer/sets. This suggests that the *16SrRNA* gene was not amplified.

3.3.5 Primer and Probe Combinations that Demonstrated Amplification

A total of 5 primer and probe combinations showed amplification of the expected target size suggesting that they are amplifying the gene of interest (Table 2). These primer and probe combinations will be further utilized on the cDNA samples in qPCR.

Table 2. Primer and probe combinations selected for quantitative polymerase chain reaction (qPCR).

Target Gene	Primer/Probe Combination
kgp	80F/123P/183R 362F/390P/437R 2436F/2457P/2516R
hmuY	384F/416P/513R
narG	2383F/2438P/2515R

4 DISCUSSION

This study designed and validated primers and probes for qPCR to assess the expression levels of *hmuY*, *kgp*, and *narG* in human oral microbiome cDNA samples. Quantitative polymerase chain reaction (qPCR) allows us to not only amplify regions of DNA but to quantify abundance of specific genes in a sample. We found that *hmuY*, *kgp*, and *narG* were amplified of correct size in the positive control samples (100 ng/µL stock *P. gingivalis*, AlphaDNA), suggesting that the primer targets are accurate. This work will lay foundation for quantifying the absolute abundance of *P. gingivalis* and the expression levels of *hmuY*, *kgp*, and *narG* in the cDNA samples using qPCR, and, overall, how nitrate supplementation affects these abundances. Additionally, results from the qPCR analysis will give us more precise measurements of how much *Porphyromonas sp.* are present in the samples which can then be compared to the physiological responses to nitrate supplementation from the study conducted by Freeze et al. (2022). A reduction of *P. gingivalis* in the oral microbiome could lower the risk of periodontitis and Alzheimer's disease and improve various cardiovascular and physiological responses.

4.1 Primer Design

Quantitative polymerase chain reaction (qPCR) is a tool used for analysis and quantification of gene expression. It is advantageous because data can be viewed in real time using a computer; a fluorescent dye is incorporated via a probe which intercalates with the amplified region of interest (Thornton and Basu 2015; Higuchi et al. 1993). The most common probe systems used today are Molecular Beacon®, SYBR Green®, and Taqman®; however, the success of qPCR amplfication and quantification are dependent on primers and probes used (Thornton and Basu 2015). Geneious Prime is a program for testing the design and specificity of primer pairs for qPCR for use in low- to high-throughput transcript profiling experiments (Arvidsson et al. 2008; Higuchi et al. 1993). Considerations for primer design in this study include GC content (approximately 50%), target size of amplicon (50-150 bp), length (18-21 nucleotides, and melting temperature (60-80°C). Other parameters such as primer self-dimer and secondary structure formation are also important considerations (Thornton and Basu 2015).

4.1.1 *kgp* and *hmuY*

Kgp inhibitors block the acquisition of host heme by *P. gingivalis* (Smalley et al. 2007). Results from the agarose gel for *kgp* show presence of amplified regions of target sizes in the positive control lanes for three primer/sets tested – 80F/183R, 362F/437F, and 2436F/2516R. This suggests that the *kgp* gene was amplified using all three sets (Figure 7). *hmuY* is the gene responsible for heme acquisition in *P. gingivalis*. Results from the agarose gel for *hmuY* show presence of an amplified region of target size in the positive control lane for one of the primer/sets tested – 384F/513R. This suggests that the *hmuY* gene was amplified using this set. Sanger sequencing on the gel band can be done to confirm its identity and the specificity of the primers (Figure 8).

4.1.2 *narG*

Gene sequences related to the enzymes involved in nitrate reduction (*napA, narG, nirK, nirS, nosZ, nrfA*) have been isolated and have been shown to differ significantly from previously recorded sequences (Papaspyrou, 2014). A study conducted by Papaspyrou et al. suggested that NAR was proportionally more important than NAP and can be more easily targeted with qPCR probes (2014). Results from the agarose gel for *narG* show presence of an amplified region of target size in the positive control lane (*P. gingivalis* stock; Alpha DNA) for one of the primer/sets – 2383F/2515R. This suggests that the *narG* gene was amplified using this set. Sanger sequencing on the gel band can be done to confirm its identity and the specificity of the primers (Figure 9).

4.1.3 *16SrRNA*

Results from the agarose gel does not show presence of amplified regions of target size in the positive control lane (*P. gingivalis* stock; Alpha DNA) for any of the primer/sets. This suggests that the *16SrRNA* gene was not amplified. The *16SrRNA* gene is one that is present in all prokaryotic life, so it was expected that we could amplify this gene in the clinical samples. However, there are a couple of reasons that can be speculated as to why we could not obtain amplified product. When compiling sequences for the *16SrRNA* gene for *P. gingivalis* only one strain was acquired. This increases the specificity of the primer; however, it decreases the likelihood of targeting the strain of *P. gingivalis* present in the samples meaning that it is likely that the specific strain is not present and was not amplified. It is also possible that the concentration of *P. gingivalis* is too low in the samples and cannot be amplified with the chosen primer sets.

4.2 Conclusions and Future Work

Identifying potential treatments and preventative measures for AD is becoming of increasing concern with its more prevalent detection worldwide. Links between oral health and overall health are also being studied to a greater degree; *Porphyromonas gingivalis* is a bacterium that exists in the oral cavity and has been linked to AD pathology (Dominy et al. 2019). A dietary nitrate supplement has been suggested to reduce the abundance of *P. gingivalis* in the oral cavity, and, thus, potentially provide protection against the progression of AD in individuals (Dominy et al. 2019). In the previous study, significant differences in vascular health, oral microbiome composition, or the abundance of *Porphyromonas* after a 10-day nitrate were not observed (Freeze et al. 2022). However, it was found that the microbiome associated with each sample type was closely related among individuals, the oral microbiome composition remains relatively stable over time, and the largest relative abundance of *Porphyromonas sp.* is found in floss samples as compared to other sample types (Freeze et al. 2022). With the methodology presented here, it is hypothesized that we can increase the specificity of the assay and obtain more precise measurements of the absolute abundance of *P. gingivalis* in the samples as well as the expression levels of *hmuY, kgp,* and *narG* which are key players in the metabolism of *P. gingivalis* and nitrate reduction. This has the potential to be developed into a larger scale study where we could pursue a larger sample size and explore the usage of different nitrate sources to provide further insight into how vascular health and the oral microbiome respond to chronic nitrate supplementation. This study designed novel primers and probes to specifically target *kgp, hmuY, and narG* in response to in vivo nitrate supplementation which opens up new avenues of research with regard to the aforementioned genes and *P. gingivalis*. Studies can be conducted to assess the effects of nitrate supplementation on those individuals with Alzheimer's disease to see if there is a link between

oral microbiome dysbiosis and cognitive impairment. If future studies see improvements post nitrate supplementation in overall health, the use of a dietary nitrate supplement could potentially be administered to people suffering from cognitive impairment, with the hope of it reducing the symptoms of Alzheimer's disease.

5 LITERATURE CITED

Anand KS, Dhikav V. 2012. Hippocampus in health and disease: An overview. Ann Indian Acad Neurol. 15(4): 239-246. doi: 10.4103/0972-2327.104323.

Armstrong RA. 2013. What causes Alzheimer's disease? Folia Neuropathol. 51(3): 169-188. doi: 10.5114/fn.2013.37702.

Arvidsson S, Kwasniewski M, Riaño-Pachón DM, Mueller-Roeber B. 2008. QuantPrime – a flexible tool for reliable high-throughput primer design for quantitative PCR. BMC Bioinformatics 9(465). doi: 10.1186/1471-2105-9-465

Beydoun MA, Beydoun HA, Hossain S, El-Hajj ZW, Weiss J, Zonderman AB. 2020. Clinical and Bacterial Markers of Periodontitis and Their Association with Incident All-Cause and Alzheimer's Disease Dementia in a Large National Survey. J Alzheimer's Dis. 75(1): 157-172. doi: 10.3233/JAD-200064.

Chen, G, Xu T, Yan Y, Zhou Y, Jiang Y, Melcher K, Xu HE. 2017. Amyloid beta: structure, biology and structure-based therapeutic development. Acta Pharmacol Sin. 38: 1205-1235. doi: 10.1038/aps.2017.28.

d'Errico P, Meyer-Luehmann M. 2020. Mechanisms of Pathogenic Tau and Aβ Protein Spreading in Alzheimer's Disease. Front Aging Neurosci. 12: 265. doi: 10.3389/fnagi.2020.00265.

de Bruijn RF, Ikram MA. 2014. Cardiovascular risk factors and future risk of Alzheimer's disease. BMC Med. 12: 130. doi: 10.1186/s12916-014-0130-5.

Dejam A, Hunter CJ, Schechter AN, Gladwin MT. 2004. Emerging role of nitrite in human biology. Blood Cells Mol Dis. 32(3): 423-429. doi: 10.1016/j.bcmd.2004.02.002.

Dominy SS, Lynch C, Ermini F, Benedyk M, Marczyk A, Konradi A, Nguyen M, Haditsch U, Raha D, Griffin C, et al. 2019. *Porphyromonas gingivalis* in Alzheimer's disease brains: Evidence for disease causation and treatment with small-molecule inhibitors. Sci Adv. 5(1): 122. doi: 10.1126/sciadv.aau3333.

Freeze GE, Reudink M, Bottos EM, Rakobowchuk ME. 2022 The effect of nitrate supplementation on *Porphyromonas gingivalis* abundance in the oral microbial community. Honours Thesis. unpublished.

Glenner GG, Wong CW. 1984. Alzheimer's disease: initial report of the purification and characterization of a novel cerebrovascular amyloid protein. Biochem Biophys Res Commun. 120(3): 885-890. doi: 10.1016/s0006-291x(84)80190-4.

Gosztyla ML, Brothers HM, Robinson SR. 2018. Alzheimer's Amyloid-β is an Antimicrobial Peptide: A Review of the Evidence. J Alzheimers Dis. 62(4): 1495-1506. doi: 10.3233/JAD-171133.

Guo Y, Nguyen K, Potempa J. 2010. Dichotomy of gingipains action as virulence factors: from cleaving substrates with the precision of a surgeon's knife to a meat chopper-like brutal degradation of proteins. Periodontal. 54(1): 15-44. doi: 10.1111/j.1600-0757.2010.00377.x.

Higuchi R, Fockler C, Dollinger G, Watson R. 1993. Kinetic PCR analysis: real-time monitoring of DNA amplification reactions. Nat Biol Technol. 11: 1026-1030.

Ide M, Harris M, Stevens A, Sussams R, Hopkins V, Culliford D, Fuller J, Ibbett P, Raybould R, Thomas R, et al. 2016. Periodontitis and Cognitive Decline in Alzheimer's Disease. PLoS One. 11(3): e0151081. doi: 10.1371/journal.pone.0151081.

Ishida N, Ishihara Y, Ishida K, Tada H, Funaki-Kato Y, Hagiwara M, Ferdous T, Abdullah M, Mitani A, Michikawa M, et al. 2017. Periodontitis induced by bacterial infection exacerbates features of Alzheimer's disease in transgenic mice. NPJ Aging Mech Dis. 3:15. doi: 10.1038/s41514-017-0015-x.

Kamer AR, Craig RG, Dasanayake AP, Brys M, Glodzik-Sobanska L, de Leon MJ. 2008. Inflammation and Alzheimer's disease: possible role of periodontal diseases. Alzheimer's Dement. 4(4): 242-250. doi: 10.1016/j.jalz.2007.08.004.

Kametani F, Hasegawa M. 2018. Reconsideration of Amyloid Hypothesis and Tau Hypothesis in Alzheimer's Disease. Front Neurosci. 12: 25. doi: 10.3389/fnins.2018.00025.

Kanagasingam S, Chukkapalli SS, Welbury R, Singhrao SK. 2020. *Porphyromonas gingivalis* is Strong Risk Factor for Alzheimer's Disease. J Alzheimer's Dis Rep. 4(1): 501-511. doi: 10.3233/ADR-200250.

Kelleher RJ, Soiza RL. 2013. Evidence of endothelial dysfunction in the development of Alzheimer's disease: Is Alzheimer's a vascular disorder? Am J Cardiovasc Dis. 3(4): 197-226.

Kinane DF, Stathopoulou PG, Papapanou PN. 2017. Periodontal diseases. Nat Rev Dis Primers. 3: 17038. doi: 10.1038/nrdp.2017.38.

Kumar DK, Choi SH, Washicosky KJ, Eimer WA, Tucker S, Ghofrani J, Lefkowitz A, McColl G, Goldstein LE, Tanzi RE, et al. 2017. Amyloid-β peptide protects against microbial infection in mouse and worm models of Alzheimer's disease. Sci Transl Med. 8(340): 340ra72. doi: 10.1126/scitranslmed.aaf1059.

Lamont RJ, Jenkinson HF. 1998. Life below the gum line: pathogenic mechanisms of *Porphyromonas gingivalis.* Microbiol Mol Biol Rev. 62(4): 1244-1263. doi: 10.1128/MMBR.62.4.1244-1263.1998.

Leira Y, Dom.nguez C, Seoane J, Seoane-Romero J, P.as-Peleteiro JM, Takkouche B, Blanco J, Aldrey JM. 2017. Is Periodontal Disease Associated with Alzheimer's Disease? A Systematic Review with Meta-Analysis. Neuroepidemiology. 48(1-2): 21-31. doi:10.1159/000458411.

Lundberg J, Weitzberg E, Gladwin M. 2008. The nitrate–nitrite–nitric oxide pathway in physiology and therapeutics. Nat Rev Drug Discov. 7: 156–167. doi: 10.1038/nrd2466.

Medeiros R, Baglietto-Vargas D, LaFerla FM. 2011. The role of tau in Alzheimer's disease and related disorders. CNS Neurosci Ther. 17(5): 514-524. doi: 10.1111/j.1755-5949.2010.00177.x.

Moen AE, Tann.s TM, Vatn S, Ricanek P, Vatn MH, Jahnsen J, IBD-Character Consortium. 2016. Simultaneous purification of DNA and RNA from microbiota in a single colonic mucosal biopsy. BMC Res Notes. 9: 328. doi: 10.1186/s13104-016-2110-7.

Murphy MP, LeVine H III. 2010. Alzheimer's disease and the amyloid-beta peptide. J Alzheimer's Dis. 19(1): 311-23. doi: 10.3233/JAD-2010-1221.

NIH Human Microbiome Project – Core Microbiome Sampling Protocol. 2010. Human Microbiome Project Consortium. https://www.ncbi.nlm.nih.gov/projects/gap/cgibin/document.cgi?study_id=phs000228.v3.p1&phd=3190#sec1

Papaspyrou S, Smith CJ, Dong LF, Whitby C, Dumbrell AJ, Nedwell DB. 2014. Nitrate reduction functional genes and nitrate reduction potentials persist in deeper estuarine sediments. Why? PLoS One. 9(4). doi: 10.1371/journal.pone.0094111

Raji CA, Lopez OL, Kuller LH, Carmichael OT, Becker JT. 2009. Age, Alzheimer disease, and brain structure. Neurology. 73(22): 1899-905. doi: 10.1212/WNL.0b013e3181c3f293.

Romitelli F, Santini SA, Chierici E, Pitocco D, Tavazzi B, Amorini AM, Lazzarino G, Di Stasio E. 2007. Comparison of nitrite/nitrate concentration in human plasma and serum samples measured by the enzymatic batch Griess assay, ion-pairing HPLC and ion-trap GC-MS: the importance of a correct removal of proteins in the Griess assay. J Chromatogr B Analyt Technol Biomed Life Sci. 851(1-2): 257-267. doi: 10.1016/j.jchromb.2007.02.003.

Rosier BT, Buetas E, Moya-Gonzalvez EM, Artacho A, Mira A. 2020. Nitrate as a potential prebiotic for the oral microbiome. Sci Rep. 10(1): 1-15. doi: 10.1038/s41598-020-69931-x.

Santos CY, Snyder PJ, Wu WC, Zhang M, Echeverria A, Alber J. 2017. Pathophysiologic relationship between Alzheimer's disease, cerebrovascular disease, and cardiovascular risk: A review and synthesis. Alzheimer's Dement. 7: 69-87. doi: 10.1016/j.dadm.2017.01.005.

Sheets SM, Potempa J, Travis J, Casiano CA, Fletcher HM. 2005. Gingipains from *Porphyromonas gingivalis* W83 induce cell adhesion molecule cleavage and apoptosis in endothelial cells. Infect Immun. 73(3): 1543-1552. doi: 10.1128/IAI.73.3.1543-1552.2005.

Singhrao SK, Harding A, Poole S, Kesavalu L, Crean S. 2015. *Porphyromonas gingivalis* periodontal infection and its putative links with Alzheimer's disease. Mediators Inflamm. 137357. doi: 10.1155/2015/137357.

Singhrao SK, Harding A. 2020. Is Alzheimer's disease a polymicrobial host microbiome dysbiosis? Expert Rev Anti Infect Ther. 18(4): 275-277. doi: 10.1080/14787210.2020.1729741.

Smalley JW, Birss AJ, Szmigielski B, Potempa J. 2007 Sequential action of R- and K-specific gingipains of *Porphyromonas gingivalis* in the generation of the heam-containing pigment from oxyhaemoglobin. Arch Biochem Biophys. 465(1): 44-49. doi: 10.1016/j.abb.2007.05.011

Thornton B, Basu C. 2015. Rapid and simple method of qPCR primer design. Methods Mol Biol. 1275: 173-179. doi: 10.1007/978-1-4939-2365-6_13

Vanhatalo A, Blackwell JR, L'Heureux JE, Williams DW, Smith A, van der Giezen M, Winyard PG, Kelly J, Jones AM. 2018. Nitrate-responsive oral microbiome modulates nitric oxide homeostasis and blood pressure in humans. Free Radic Biol Med. 124(3): 21-30. doi: 10.1016/j.freeradbiomed.2018.05.078.

Wylie LJ, Kelly J, Bailey SJ, Blackwell JR, Skiba PF, Winyard PG, Jeukendrup AE, Vanhatalo A, Jones AM. 2013. Beetroot juice and exercise: pharmacodynamic and dose-response relationships. J Appl Physiol. 115(3): 325-336. doi: 10.1152/japplphysiol.00372.2013.

6 APPENDIX

Table 4. RNA concentrations of floss samples analyzed in this study (n=20).

Sample Name	RNA Concentration (ng/µL)
P01 Pre-F	tl
P02 Pre-F	5.15
P03 Pre-F	3.84
P04 Pre-F	3.29
P05 Pre-F	10.80
P06 Pre-F	3.58
P07 Pre-F	10.40
P08 Pre-F	tl
P09 Pre-F	7.36
P10 Pre-F	9.42
P01 Post-F	2.40
P02 Post-F	3.64
P03 Post-F	12.30
P04 Post-F	2.10
P05 Post-F	8.33
P06 Post-F	2.98
P07 Post-F	4.20
P08 Post-F	tl
P09 Post-F	16.20
P10 Post-F	23.50

P01-P10 denotes participant number; Pre-F denotes the floss samples taken pre-supplementation; Post-F denotes the floss samples taken post-supplementation; tl = too low to quantify (<0.05 ng/µL)